HHS Public Access

Author manuscript

Biochemistry. Author manuscript; available in PMC 2015 December 10.

Published in final edited form as:

Biochemistry. 2015 June 30; 54(25): 3880–3889. doi:10.1021/bi5014497.

Frataxin Accelerates [2Fe-2S] Cluster Formation on the Human Fe–S Assembly Complex

Nicholas G. Fox[†], **Deepika Das**[†], **Mrinmoy Chakrabarti**[†], **Paul A. Lindahl**[†,‡], and **David P. Barondeau**[*,†]

[†]Department of Chemistry, Texas A&M University, College Station, Texas 77843-3255, United States

[‡]Department of Biochemistry and Biophysics, Texas A&M University, College Station, Texas 77843-2128, United States

Abstract

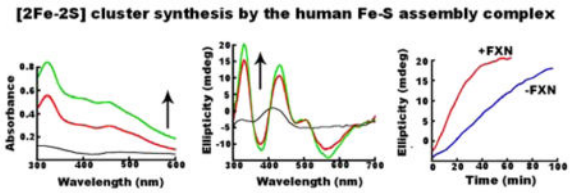

Iron–sulfur (Fe–S) clusters function as protein cofactors for a wide variety of critical cellular reactions. In human mitochondria, a core Fe–S assembly complex [called SDUF and composed of NFS1, ISD11, ISCU2, and frataxin (FXN) proteins] synthesizes Fe–S clusters from iron, cysteine sulfur, and reducing equivalents and then transfers these intact clusters to target proteins. *In vitro* assays have relied on reducing the complexity of this complicated Fe–S assembly process by using surrogate electron donor molecules and monitoring simplified reactions. Recent studies have concluded that FXN promotes the synthesis of [4Fe-4S] clusters on the mammalian Fe–S assembly complex. Here the kinetics of Fe–S synthesis reactions were determined using different electron donation systems and by monitoring the products with circular dichroism and absorbance spectroscopies. We discovered that common surrogate electron donor molecules intercepted Fe–S cluster intermediates and formed high-molecular weight species (HMWS). The HMWS are associated with iron, sulfide, and thiol-containing proteins and have properties of a heterogeneous solubilized mineral with spectroscopic properties remarkably reminiscent of those of [4Fe-4S] clusters. In contrast, reactions using physiological reagents revealed that FXN accelerates the formation of [2Fe-2S] clusters rather than [4Fe-4S] clusters as previously reported. In the

[*]Corresponding Author: Department of Chemistry, Texas A&M University, College Station, TX 77843-3255. barondeau@tamu.edu. Telephone: (979) 458-0735. Fax: (979) 458-0736.

Author Contributions

N.G.F. and D.D. contributed equally to this work.

Notes

The authors declare no competing financial interest.

Supporting Information

Results of additional experiments on the formation and properties of HMWS. The Supporting Information is available free of charge on the ACS Publications website at DOI: 10.1021/bi5014497.

preceding paper [Fox, N. G., et al. (2015) *Biochemistry 54*, DOI: 10.1021/bi5014485], [2Fe-2S] intermediates on the SDUF complex were shown to readily transfer to uncomplexed ISCU2 or apo acceptor proteins, depending on the reaction conditions. Our results indicate that FXN accelerates a rate-limiting sulfur transfer step in the synthesis of [2Fe-2S] clusters on the human Fe–S assembly complex.

Proteins containing iron–sulfur (Fe–S) clusters are involved in many critical functions in cells, including oxidative respiration, DNA replication and repair, and cofactor biosynthesis.[1] Sophisticated Fe–S assembly pathways synthesize and deliver Fe–S clusters to apo target proteins.[2–7] These O_2-sensitive pathways involve more than a dozen proteins and require six substrates to generate the simplest (i.e., [2Fe-2S]) cluster. Numerous protein complexes are assembled and disassembled during cluster formation and transfer reactions.

Because of this complexity, assays for investigating the mechanistic enzymology of these pathways have had to simplify this process by including nonphysiological reagents and by monitoring partial reactions. An additional challenge is that iron and sulfide can undergo competing nonenzymatic Fe–S cluster self-assembly (spontaneous formation of discrete species similar to biological Fe–S clusters)[8] and Fe–S mineralization chemistry. The resulting Fe–S material can also undergo ligand exchange and cluster conversion reactions (DOI: 10.1021/bi5014485). It is important to elucidate the factors that partition between biosynthetic and competing side reactions and to understand the types and properties of Fe–S species that are being generated.

The mitochondrial eukaryotic Fe–S biosynthetic pathway builds Fe–S clusters from the substrates L-cysteine, iron, and reducing equivalents, homologous to the chemistry of the prokaryotic ISC pathway. Cysteine desulfurase (human NFS1 or bacterial IscS) catalyzes the PLP-dependent conversion of L-cysteine to L-alanine, while generating a persulfide species on a mobile loop cysteine that delivers a sulfane sulfur to the Fe–S catalytic protein (human ISCU2 or bacterial IscU).[9,10] Cysteine desulfurase activity is often measured by intercepting this persulfide species using reductive thiol-cleaving reagents and quantitating the generated sulfide.[9–11] Human NFS1 forms a tight complex with ISD11 (the SD complex) that includes two NFS1 and possibly four ISD11 subunits.[12] ISD11 is a eukaryotic protein that stabilizes cysteine desulfurase and may help position the mobile loop cysteine for attack of the substrate.[13–15] Possible electron donors for *in vivo* Fe–S cluster formation and/or transfer include glutathione (GSH) and NADPH with the ferredoxin/ferredoxin reductase system.[16–18] Notably, *in vitro* Fe–S cluster assembly reactions often use a surrogate electron donor such as dithiothreitol (DTT). Once the Fe–S clusters are assembled, chaperone and Fe–S carrier proteins facilitate the transfer of the intact Fe–S clusters from the Fe–S assembly complex to target proteins.[19–21]

Depletion of human frataxin (FXN) is associated with the loss of Fe–S cluster enzyme activities and the development of the neurodegenerative disease Friedreich's ataxia (FRDA).[22] FXN binds to an ~160 kDa complex consisting of NFS1, ISD11, and ISCU2 proteins (named SDU) to form the SDUF complex.[12,23] FXN was initially proposed to function as an iron donor for Fe–S cluster biosynthesis largely because of its ability to weakly bind iron.[24–26] Subsequently, FXN was shown to stimulate the activity of the

cysteine desulfurase component of the SDUF complex (k_{cat} is ~10-fold higher for SDUF than for SDU), suggesting a role as an allosteric effector.[23,27–29] Notably, FXN variants encoded by FRDA missense mutations have compromised abilities to bind and stimulate the activities of the Fe–S assembly complex.[30,31] Recent Mössbauer studies suggest that the mouse SDU complex assembles [2Fe-2S] clusters and that the SDUF complex synthesizes [4Fe-4S] clusters.[32] This result is puzzling because an IscU molecule in the SDUF complex would not be expected to dimerize (a requirement for the reductive coupling model of [4Fe-4S] cluster formation)[33] without a significant conformational change compared to the prokaryotic IscS–IscU structure. In addition, proteins previously implicated in [4Fe-4S] cluster formation[34] were not added during the reaction, and the putative [4Fe-4S] cluster was EPR silent under both oxidized and reduced conditions.

The objectives of this study were to elucidate the formation kinetics and types of Fe–S clusters synthesized by the human Fe–S assembly complex under different experimental conditions. Previous kinetic assays for Fe–S cluster formation used the surrogate electron donor DTT and followed the increase in absorbance at 456 nm due to S → Fe charge transfer bands.[23,35–37] This wavelength is characteristic of an absorbance peak for [2Fe-2S] clusters, but other Fe–S species, including [4Fe-4S] clusters, also absorb there. Under these assay conditions, the SDUF complex exhibited activity ~25-fold higher than that of the SDU complex.[23] However, the nature of the Fe–S species produced during these assembly reactions were not determined. In this paper and the preceding paper (DOI: 10.1021/bi5014485), different electron donation systems were used for Fe–S cluster assembly reactions and the products of these reactions were established using electronic absorbance, circular dichroism, and Mössbauer spectroscopies. Together, they reveal new details of the Fe–S cluster assembly reaction on the SDUF complex and of competing Fe–S cluster conversion and mineralization chemistry that have implications for the mechanism and study of Fe–S cluster biosynthesis.

MATERIALS AND METHODS

Protein Expression and Purification

NFS1-ISD11 (named SD), ISCU2, and FXN were purified as described previously.[23] The SDUF complex exhibited a cysteine desulfurase activity of 11 mol of sulfide (mol of PLP)$^{-1}$ min^{-1}, which is similar to reported values.[23,38] Briefly, plasmids that contain the genes for human SD, ISCU2, and FXN were individually transformed into BL21(DE3) cells. Cells were grown at 37 °C until an OD_{600} of 0.6 was achieved. Protein expression was induced with either 0.5 mM (ISCU2 and FXN) or 0.1 mM (SD) IPTG; the temperature was reduced to 16 °C, and the cells were harvested 16 h later. Plasmid PET9a encoding human ferredoxin (FDX1, gift of J. Markley)[39] was transformed into *Escherichia coli* BL21(DE3) cells and grown at 37°C until an OD_{600} of 0.6 was reached. Expression was induced with 0.4 mM IPTG, 1 mM cysteine, and 0.1 mg/mL ferric ammonium citrate, and the cells were harvested 16 h later. Buffer A [50 mM HEPES (pH 7.8) and 250 mM NaCl] was used for all experiments unless otherwise stated. The cells were lysed by sonication, and the soluble proteins were loaded onto an anion exchange column (26/20 POROS 50HQ, Applied Biosystems) and eluted with a linear gradient from 0 to 1000 mM NaCl in 50 mM Tris (pH

7.5). Fractions containing FDX1 were further purified[40] on a Sephacryl S100 (26/60, GE Healthcare) size-exclusion column equilibrated in 50 mM Tris (pH 7.4) and 50 mM NaCl. Apo-FDX1 was prepared by incubating purified FDX1 with 10 mM DTT, adding 10% trichloroacetic acid on ice for 10 min, pelleting the sample, rinsing the pellet twice with water, and resuspending the pellet anaerobically in 50 mM Tris (pH 8.0) and 250 mM NaCl.[40] Anaerobic experiments were performed in an Mbraun glovebox at ~12 °C with an argon atmosphere and <1 ppm O_2 as monitored by a Teledyne model 310 analyzer.

Fe–S Cluster Formation Assays

The Fe–S cluster assembly assay mixtures under two experimental conditions (standard and DTT-free) were prepared anaerobically and transferred to a 1 cm path length anaerobic cuvette for UV–visible (Agilent UV–visible 8453) and circular dichroism (CD) (Chirascan) data collection at 20 °C. Standard assay conditions include 10 μM SD, 30 μM ISCU2, 30 μM FXN with 4 mM DTT, 100 μM cysteine, and either 250 or 400 μM $Fe(NH_4)_2(SO_4)_2$. Final volumes were 250 μL for UV–visible-based and 200 or 400 μL for CD-based assays. DTT-free conditions were the same as standard conditions except that (a) the L-cysteine concentration was increased to 1 mM, (b) samples lacked DTT, and (c) the $Fe(NH_4)_2(SO_4)_2$ concentration was decreased from 400 to 250 μM. The initial linear regions for the SDU and SDUF reactions under DTT-free conditions were fit using KaleidaGraph (Synergy Software). For the sulfide addition experiments, the development of the [2Fe-2S] cluster using 50 μM ISCU2 was monitored with anaerobic CD spectroscopy under DTT-free conditions. Once the CD signal at 330 nm had been maximized (indicating the development of the [2Fe-2S] species), aliquots of a Na_2S stock solution were added to final Na_2S concentrations of 250, 500, and 1000 μM and the CD spectra were immediately measured.

Protein Assembly State Analysis

Sample mixtures of 50 μM SD and 150 μM ISCU2 with (SDUF) or without (SDU) 150 μM FXN were incubated anaerobically for 20 min at 10 °C with 1.5 mM DTT, 500 μM $Fe(NH_4)_2(SO_4)_2$, and 500 μM L-cysteine (complete reaction conditions). Additional reactions lacking DTT, $Fe(NH_4)_2(SO_4)_2$ and/or L-cysteine were also prepared. Samples were applied to an anaerobic S-200 column (Superdex 200 10/300 GL, GE Healthcare) equilibrated with buffer A. In a second set of experiments, NFS1 was alkylated by incubating 50 μM SD with 1 mM iodoacetamide for 1 h at 12 °C and quenched with 10 mM cysteine. Modification of NFS1 residue C381 was confirmed by mass spectrometry. Alkylated or nonalkylated SD was reacted for 15 min at 12 °C with 50 μ M ISCU2, 50 μM FXN, 200 μM $Fe(NH_4)_2(SO_4)_2$, 1.5 mM DTT, and 200 μM Na_2S (final concentrations, 0.2–0.5 mL reaction volume) and applied to the S-200 column. In a third set of experiments, 100 μM SDUF (final concentration) was prepared by mixing 100 μM SD, 300 μM ISCU2, 300 μM FXN, 1 mM $Fe(NH_4)_2(SO_4)_2$, and 3 mM DTT in the presence and absence of 500 μM apo-FDX1. The reaction was initiated with 1 mM L-cysteine (final concentration, 0.2–0.5 mL reaction volume). After reacting for 45 min at 12 °C, the solution was applied to an S-200 column. The reaction without apo-FDX1 was repeated, and the high-molecular weight species (HMWS) was isolated from fractions of the S-200 column. The HMWS sample was split, and half was incubated for 10 min with 4 mM DTT. The other half was incubated for 40 min with 500 μM apo-FDX1 and 4 mM DTT. Samples were then reapplied to an S-200

column. Calibration with molecular weight standards confirmed that the protein samples eluted at volumes corresponding to their known molecular masses. Sulfide production was measured using a methylene blue assay.[23,41,42] Iron was quantified by the ferrozine assay.[43–45]

Mössbauer Analysis of HMWS

Mössbauer samples of HMWS were prepared by reacting 600 μM SD or SDUF with 6 mM L-cysteine, 6 mM ^{57}Ferric citrate, and 1.8 mM DTT for 45 min at 12 °C, and isolating the HMWS using an S-200 column equilibrated in buffer A. Mössbauer spectra were recorded using a model MS4 WRC spectrometer (SEE Co., Edina, MN) at 0.05 T applied parallel to the γ radiation. Spectra were analyzed using WMOSS software (SEE Co.). Parameters are quoted relative to α-Fe foil at 298 K.

RESULTS

Fe–S cluster assembly reaction components were prepared anaerobically in a glovebox and combined in an anaerobic cuvette that was sealed with a rubber septum and removed from the glovebox for activity measurements. Activity assays were initiated by injecting L-cysteine into the sealed cuvette using a gastight syringe. We employed two types of Fe–S assembly assay conditions, called standard and DTT-free (see Materials and Methods), that differed in their electron donation systems. We first investigated the Fe–S cluster assembly reaction for the SDUF complex (with an SD:ISCU2:FXN molar ratio of 1:3:3) under standard assay conditions, which included substrates Fe^{2+} and L-cysteine, and electron donor DTT. After 1 h, the reaction mixture exhibited a broad peak with a maximum at 400 nm that is characteristic of [4Fe-4S] clusters[46] (Figure 1A). In addition, the absorbance for the entire visible region increased with time. The origin of the general absorbance increase at all wavelengths is unclear, but it is consistent with an increase in light scattering. The absorbance at 400 nm increased rapidly and then more slowly in a second linear phase of the reaction (Figure 1B). The rate and magnitude of the absorbance changes depended on the concentration of Fe^{2+} (data not shown). The lack of a plateau region indicates that more than one reaction occurred and/or that more than one species formed. None of the spectra recorded, even at the earlier reaction times, showed absorbance features typical of a [2Fe-2S] cluster. The corresponding CD spectra exhibited a feature at 420 nm that was largely invariant with time (Figure 1C). This feature was assigned to the PLP cofactor, as a similar peak was observed for the human SD complex and *E. coli* IscS that lack iron–sulfur clusters. The intensity of a second CD peak at 300 nm decreased with time. The iron independence of this second feature (Figure 1D) suggested that it was also due to the PLP cofactor and not to an Fe–S cluster. Moreover, these features were inconsistent with the strong [2Fe-2S] cluster-dependent CD signals observed at 330 and 430 nm exhibited by bacterial IscU[21,47,48] and human ISCU2.[29] Rather, they suggested the formation of [4Fe-4S] clusters, which have negligible UV–visible CD intensity compared to that of [2Fe-2S] clusters.[49,50] These features could also be due to other Fe–S species (such as an Fe–S mineral) that exhibit similar absorbance and CD spectroscopic properties.

We repeated the Fe–S cluster assembly reaction under standard conditions in the absence of FXN (SDU complex with an SD:ISCU2 molar ratio of 1:3). As previously reported,[23] the absorbance increase at 456 nm for the SDU complex was significantly slower than that of the SDUF complex. The plot was linear and was not maximized during the time frame of the experiment (Figure 2A, black line). Early time points for the SDU reaction revealed spectral absorption features typical of a [2Fe-2S] cluster (Figure 2B). The formation of a [2Fe-2S] cluster was further supported by the development of a strong CD signal with peaks at 330 and 430 nm that are characteristic of [2Fe-2S]-IscU (Figure 2C). Absorbance features centered at 400 nm and an overall increase at all wavelengths (Figure 2B) developed at later times, similar to those produced by SDUF reactions.

Time-dependent changes in the 330 nm CD signal of a separate SDU sample under standard conditions were monitored. The signal plateaued after ~30 min and then decreased back to the initial ellipticity value (Figure 2D). This is consistent with the SDU complex generating a [2Fe-2S] cluster that converts into a different species lacking a significant CD signature. The cluster conversion chemistry appears to vary with cysteine desulfurase activity and the amount of sulfide produced (see below). Overall, these results suggest that multiple species are generated in Fe–S assembly reactions under standard conditions.

Fe–S Cluster Assembly Reactions under Standard Conditions Generate High-Molecular Weight Species (HMWS)

Human SDU and SDUF complexes were isolated and characterized from similar assembly reactions. Standard reaction conditions were used (except for higher protein concentrations), and products were analyzed by anaerobic analytical size-exclusion chromatography. A brown species eluted in the column void volume (at ~9 mL) when either SDU (Figure 3A) or SDUF (Figure 3B) complexes were used. SD, SDU, and SDUF complexes eluted at ~12 mL, and uncomplexed ISCU2 and FXN eluted at ~16 mL. Forming this HMWS required Fe^{2+}, L-cysteine, and the assembly complex. The reaction was accelerated by DTT (data not shown). Sodium dodecyl sulfate–polyacrylamide gel electrophoresis (SDS–PAGE) analysis of fractions containing SDU (Figure 3C) and SDUF (Figure 3D) indicated that the HMWS (fraction 9 in each case) contained SD and ISCU2. Most of the iron and sulfide added in the reaction mixture eluted with the HMWS. More iron and sulfide (9 Fe^{2+} and 10 S^{2-} atoms per SDU assuming a 1:2:1 stoichiometry[12]) were found in the HMWS fraction for the SDUF reaction than expected for a standard biological Fe–S cluster. A similar Fe–S cluster-associated HMWS could be generated in control reactions (Figure S1 of the Supporting Information) using either the SD complex or *E. coli* IscS in the absence of the scaffold protein (human ISCU2 or *E. coli* IscU). As the ISCU2/IscU protein is required for biological Fe–S cluster assembly, this suggests that HMWS formation is an off-pathway process that competes with the physiological Fe–S cluster assembly pathway under these assay conditions.

HMWS Are Solubilized Fe–S Mineral Species

We generated ^{57}Fe-labeled HMWS to investigate it by Mössbauer spectroscopy. The 5 K spectrum was composed of unresolved magnetic material and a quadrupole doublet (Figure 4A). At 100 K, the magnetic material collapsed into a doublet with $\delta = 0.37$ mm/s, $\Delta E_Q =$

0.67 mm/s, and Γ = 0.55 mm/s (Figure 4B). HMWS prepared from similar SDUF or other SD reactions displayed some spectral variability (Figure S2 of the Supporting Information), suggesting multiple species. The Mössbauer magnetic properties and parameters along with the absence of an EPR signal (with or without added dithionite) for the HMWS are inconsistent with [2Fe-2S] or [4Fe-4S] clusters. Instead, they indicate an Fe–S mineral (see Discussion).

Formation and Reaction Properties of HMWS

Next, we attempted to minimize formation of the HMWS material. We considered whether cysteine desulfurase catalyzed L-cysteine turnover and generated sulfide during HMWS formation. That sulfide could then be used in Fe–S cluster self-assembly or FeS mineralization. Consistent with this role, sulfide could be substituted for L-cysteine (Figure 5A, red line). However, alkylation of the cysteine residues of NFS1 eliminated HMWS formation even in the presence of sulfide and ferrous ions (Figure 5A, green line). This suggests that NFS1 plays an additional role in HMWS formation, e.g., as a scaffold for assembling or solubilizing an Fe–S species.

We then explored what reagent limits product formation for Fe–S cluster assembly reactions using SDUF under standard conditions (Figure 5B). The Fe–S mineral is likely responsible for the increase in both the 400 nm absorbance and the apparent light scattering. The reaction started to plateau at ~15 min, but adding L-cysteine at that point caused an abrupt rise in absorbance. This suggested that Fe–S mineral formation was limited due to depleted cysteine/sulfide, and that more of this material formed once extra cysteine was added.

We wondered whether HMWS could function as a substrate for the chemical reconstitution of apo target proteins. To test this, the SDUF reaction under standard conditions was repeated with a molar excess of the [2Fe-2S] cluster acceptor protein apo-FDX1. The reaction was analyzed by size-exclusion chromatography. An Fe–S cluster was incorporated into apo-FDX1 while less HMWS formed (Figure 5C). Incorporation of the cluster into apo-FDX1 suppressed (bypassed) formation of HMWS, or HMWS were used as reagents for building the FDX1 cluster (or both). To test the latter possibility, we purified HMWS and incubated this material with apo-FDX1 and reanalyzed it by size-exclusion chromatography (Figure 5D). Relative to the control reaction that lacked apo-FDX1, the HMWS peak intensity decreased while the peak associated with the native assembly complex increased in intensity. In addition, a peak at ~16 mL had a retention time and absorbance properties of [2Fe-2S]-FDX1. Thus, HMWS formation is reversible and can provide the iron and sulfur (perhaps after chemical transformation) to assemble a $[2Fe\text{-}2S]^{2+}$ cluster on apo-FDX1. Together, the stoichiometric, kinetic, and spectroscopic properties suggest that HMWS are heterogeneous Fe–S minerals that are solubilized by NFS1. Formation of HMWS depends on sulfide, which is readily generated by reductive cleavage of persulfide species by DTT under standard conditions.[23] Moreover, HMWS cannot be separated from the assembly complex by desalting columns, and they are capable of participating in chemical reconstitution reactions.

DTT-Free Assembly Reactions Suppress HMWS Formation

A second set of reaction conditions, called DTT-free, was used to monitor cluster biosynthesis while minimizing sulfide and HMWS generation. The absorbance spectrum of both the SDU (Figure 6A) and SDUF (Figure 6B) reaction mixtures under DTT-free conditions had features characteristic of a [2Fe-2S] cluster, rather than the broad absorption at 400 nm that was due primarily to HMWS in reaction mixtures that contained DTT (Figure 1A). In addition, the general increase in absorption at all wavelengths that was attributed to light scattering from Fe–S mineral formation was diminished. To evaluate whether HMWS were also formed, a separate SDUF Fe–S cluster assembly reaction was analyzed after incubation for 1.5 h by size-exclusion chromatography. Peaks that absorb at 405 nm for the SDUF complex and uncomplexed ISCU2 were detected (Figure 6C), but not for HMWS or low-molecular weight species (LMWS). At longer (>2 h) time points, an absorbance peak near 400 nm developed along with a general increase in absorbance at all wavelengths (Figure 6D) that was consistent with Fe–S cluster-associated HMWS formation. Initial formation of HMWS (Figure 6C, shoulder at 10–11 mL) was confirmed for the 3.5 h sample. Thus, the DTT-free reactions delayed and suppressed the rate of HMWS formation compared to standard reactions. This can be rationalized by differences in the ability of cysteine and DTT to release the sulfide from a persulfide intermediate on the assembly complex. Generation of sulfide by cysteine (DTT-free assays) occurs through an intermolecular reaction, whereas the sulfide released by DTT (standard assays) involves an entropically favored intramolecular reaction that forms a disulfide-bonded six-membered ring.

Sulfide Converts [2Fe-2S] Clusters to HMWS

Under standard conditions, the assembly reaction with SDUF failed to generate [2Fe-2S] CD signals (Figure 1C), whereas with SDU, a [2Fe-2S] CD signal developed and then slowly decayed (Figure 2D). We hypothesized that sulfide, which was generated rapidly for SDUF reactions and slowly for SDU reactions,[23] reacted with synthesized [2Fe-2S] clusters to form HMWS. To test this, an assembly reaction involving SDU and DTT-free conditions was used to generate [2Fe-2S] clusters (Figure 7A). Addition of Na_2S immediately and dramatically decreased the magnitude of the [2Fe-2S] cluster signal (Figure 7B). Lower concentrations of Na_2S resulted in partial signal loss, whereas higher concentrations completely eliminated the signal (leaving only the PLP CD feature). The addition of sulfide also resulted in an overall increase in absorbance at all wavelengths. The CD and absorbance features are similar to those observed in SDUF reactions under standard conditions and suggest that bisulfide reacts with [2Fe-2S] cluster intermediates to generate HMWS. Thus, Fe–S cluster assembly reactions that generate bisulfide are prone to competing reactions for the synthesis and degradation of [2Fe-2S] clusters (see Discussion).

FXN Binding Accelerates [2Fe-2S] Cluster Formation on ISCU2

Using DTT-free conditions that minimize the competing HMWS pathway, we assessed the role of FXN in the kinetics of [2Fe-2S] cluster formation. SDU- and SDUF-catalyzed reactions were monitored by both absorption (panels A and B of Figure 6, respectively) and CD (panels A and B of Figure 8, respectively) spectroscopies. Strong absorbance and CD

signals due to [2Fe-2S]-ISCU2 developed in both reactions, but the rates of formation were significantly more rapid in the SDUF-catalyzed reactions. Fitting the linear regions of the absorbance and CD kinetic traces (panels C and D of Figure 8, respectively) revealed that FXN enhanced the rate of [2Fe-2S]-ISCU2 cluster formation by a factor of nearly 3. The addition of FXN increased the rate of absorbance change from 4.7×10^{-4} mM/min (R^2 = 0.99) to 13.4×10^{-4} mM/min (R^2 = 0.99) (assuming an extinction coefficient of 4.58 mM^{-1} cm^{-1} at 456 nm[51]). Notably, the absorbance increase did not plateau for either reaction, consistent with the initial formation of [2Fe-2S] clusters and the generation of HMWS at later times (Figure 6C,D). In contrast, the CD intensity is more specific for protein-bound $[2Fe\text{-}2S]^{2+}$ clusters. Addition of FXN increased the rate of CD signal growth from 0.40×10^{-4} mM/min (R^2 = 0.99) to 0.97×10^{-4} mM/min (R^2 = 0.99). The CD ellipticity at 330 nm plateaued at ~20 mdeg after ~30 min for the SDUF reaction and after ~100 min for the SDU reaction (Figure 8D). The ~20 mdeg value corresponds to a [2Fe-2S] cluster concentration of ~30 μM,[21] the concentration of ISCU2 used in these experiments. Thus, the plateau in the CD intensity is consistent with the reaction halting after all of the ISCU2 in the solution became bound with [2Fe-2S] clusters. These data also indicate that these [2Fe-2S] clusters are not converted to another Fe–S species. Notably, alternate species such as Fe–S minerals (DOI: 10.1021/bi5014485), [4Fe-4S] clusters,[49,50] and [2Fe-2S] clusters associated with small molecules rather than proteins[52] do not significantly contribute to this region of the CD spectrum. Overall, these data demonstrate that adding FXN to the SDU complex increases the rate at which the complex synthesizes [2Fe-2S] clusters on ISCU2.

DISCUSSION

Experiments to identify reaction intermediates and elucidate mechanistic details of biosynthetic pathways often rely on monitoring reaction progress with kinetic measurements. This is challenging for Fe–S cluster biosynthesis researchers because the substrates (iron, cysteine, and reducing equivalents) and byproducts (sulfide) also undergo competing nonenzymatic Fe–S cluster self-assembly[8] and mineralization chemistry. Additionally, the synthesized Fe–S clusters are capable of undergoing ligand exchange and cluster conversion reactions [see the preceding paper (DOI: 10.1021/bi5014485)]. These competing reactions complicate the interpretation of results and limit mechanistic insight. It is therefore important to elucidate factors that partition reaction intermediates between these competing pathways and to understand the types and properties of Fe–S species that are being generated. Here we have identified conditions that favor pathways that intercept intermediates in Fe–S cluster biosynthesis. We have shown how to minimize this competing pathway by limiting sulfide generation and have provided insight into the reaction chemistry associated with human Fe–S cluster biosynthesis.

Fe–S cluster assembly reactions under standard conditions generated products with absorbance and CD properties consistent with [4Fe-4S] clusters. The generation of [4Fe-4S] clusters is consistent with a recent proposal for the murine FeS biosynthetic system in which FXN was proposed to have a role in generating [4Fe-4S] cluster intermediates on the assembly complex.[32] However, Mössbauer and biochemical studies revealed that reactions for the human assembly complex under similar conditions generate Fe–S mineral or high-molecular weight species (HMWS) and not [4Fe-4S] clusters. The HMWS are an iron-,

sulfide-, and protein-containing material that exhibits Mössbauer spectra with a quadrupole doublet that is similar to those of Fe–S minerals such as pyrite (δ = 0.25–0.43 mm/s, and ΔE_Q = 0.61–0.66 mm/s).[53] The Mössbauer parameters of the HMWS doublet are also similar to those assigned to [2Fe-2S]-GSH (δ = 0.393 mm/s, and ΔE_Q = 0.676 mm/s).[52] However, the spectroscopic properties of HMWS are not consistent with well-characterized $[2Fe\text{-}2S]^{2+}$ or $[4Fe\text{-}4S]^{2+}$ clusters. The former clusters generally have δ = 0.25–0.30 mm/s and ΔE_Q = 0.7–0.8 mm/s.[54] $[4Fe\text{-}4S]^{2+}$ clusters have δ = 0.44–0.46 mm/s and ΔE_Q = 0.6–1.5 mm/ s.[54] Another important difference is that the HMWS exhibit magnetic hyperfine interactions (rather than a doublet) at low temperatures. This spectral feature collapses into the doublet at higher temperatures. This behavior is distinctly different from those of $S = 0$ $[2Fe\text{-}2S]^{2+}$ or $[4Fe\text{-}4S]^{2+}$ clusters that exhibit doublets at both low and high temperatures. Also, the HMWS lack an $S = {}^1/_2$ EPR signal (with or without added dithionite). Fe–S cluster-associated HMWS have been generated during chemical reconstitution of [4Fe-4S] cluster-containing radical SAM enzymes.[55]

Standard *in vitro* Fe–S assembly reactions generate HMWS by intercepting persulfide and [2Fe-2S] cluster intermediates. In humans, a persulfide intermediate on the NFS1 component of the assembly complex is generated (Figure 9, reaction A) and transferred to ISCU2 (Figure 9, reaction B) as an initiating step in Fe–S cluster biosynthesis.[29] Addition of iron and reducing equivalents converts the terminal sulfur of this persulfide species into the bridging sulfur of a [2Fe-2S] cluster (Figure 9, reaction C).[29] Transfer of the [2Fe-2S] cluster intermediate to a target protein completes the catalytic cycle for the assembly complex (Figure 9, reaction D). Nucleophilic reagents such as surrogate electron donor DTT and the substrate cysteine can attack or intercept protein-bound persulfide intermediates to produce sulfide ions (Figure 9, reaction E). Subsequent reaction of sulfide (or bisulfide) with iron and the assembly complex generates HMWS (Figure 9, reaction F). Sulfide also appears to be capable of reacting with [2Fe-2S] intermediates and forming HMWS (Figure 9, reaction G), a process that may be accelerated by the addition of FXN. Similar thiol-based extrusion of [2Fe-2S] clusters from proteins has been reported.[56,57]

The two separate paths for forming HMWS are supported by recent kinetic studies of $SDU_{C35A}F$ and $SDU_{C61A}F$ complexes that exhibit nativelike cysteine desulfurase activities but compromised Fe–S assembly activities under standard conditions.[29] The slow increase in absorbance for $SDU_{C35A}F$ and $SDU_{C61A}F$ complexes compared to that of native SDUF is likely due to a functional persulfide cleavage pathway (Figure 9, reactions E and F) but compromised biosynthetic route (Figure 9, reactions A–C and G) to HMWS. The ISCU2 variants for the $SDU_{C35A}F$ and $SDU_{C61A}F$ complexes have mutations in the conserved cysteines used for cluster biosynthesis. These different routes to HMWS may correspond to the initial rapid (biosynthetic route) and secondary slow linear (persulfide cleavage route) changes in absorbance under standard conditions. Overall, these results indicate that Fe–S cluster assembly assays under standard (DTT-containing) conditions may be qualitatively informative (representing primarily the enzymatic [2Fe-2S] biosynthesis and degradation pathway) but are not quantitatively meaningful for measuring the rate of [2Fe-2S] cluster synthesis by the assembly complex.

We elucidated details of the human Fe–S cluster biosynthetic process by identifying reaction conditions that minimize the competing nonenzymatic pathways and by monitoring reaction progress with spectroscopic methods that are uniquely sensitive to [2Fe-2S] clusters bound to proteins. Previously, human FXN was shown to stimulate the cysteine desulfurase activity (10-fold higher k_{cat} for sulfide production)[23] and facilitate the accumulation of persulfide species on ISCU2.[29] Here, we explored the kinetics of [2Fe-2S] cluster formation under DTT-free conditions. Addition of FXN accelerated the rate of development for [2Fe-2S] CD features and resulted in approximately one [2Fe-2S] cluster per ISCU2 molecule. In the preceding paper (DOI: 10.1021/bi5014485), we show by Mössbauer spectroscopy and liquid chromatography that, under similar conditions, [2Fe-2S] clusters are present on uncomplexed ISCU2. Together, these results support a model in which FXN accelerates [2Fe-2S] cluster formation on the SDUF complex (green arrows in Figure 9, presumably using cysteine as the electron donor). This conclusion is supported by recent *in vitro* studies of a primarily *Saccharomyces cerevisiae* system in which the rate of formation for a [2Fe-2S]-Isu1 CD signal was dependent on the addition of Yfh1 (FXN homologue).[18] Interestingly, the addition of the presumed physiological electron donation system (FDX2, ferredoxin reductase, and NADPH) or nonphysiological electron donor DTT resulted in similar rates for the development of the [2Fe-2S]-Isu1 CD signal in the yeast system. This is in contrast to the human system in which the addition of DTT eliminates the [2Fe-2S]-ISCU2 CD signal. Thus, there are fundamental differences in the response of the human and yeast *in vitro* systems to surrogate electron donor DTT. In the future, these *in vitro* studies need to be expanded to evaluate complete cluster synthesis and transfer reactions that include chaperones, intermediate carrier proteins, and different Fe–S target proteins.

In summary, we have provided new details of competing pathways for Fe–S cluster biosynthesis and Fe–S mineralization. The partitioning of reaction intermediates complicates the interpretation of *in vitro* Fe–S assembly results. Deconvoluting the enzymatic and mineralization processes is challenging as there appears to be multiple partitioning branch points, comparable formation kinetics (both ultimately depend on cysteine turnover by NFS1), overlapping absorbance properties, products that co-elute on desalting columns, and similar abilities to transfer (Figure 9, reaction D) or chemically reconstitute (Figure 9, reaction H) Fe–S clusters on target proteins. In these cases, performing reactions under conditions that minimize off-pathway reactions and monitoring the kinetics with multiple interrelated spectroscopic methods may be required to elucidate mechanistic details for the assembly and/or transfer of Fe–S clusters. Together, our current and previous[23,29] results are consistent with yeast studies[18,28] and indicate that FXN accelerates a rate-limiting sulfur transfer step in [2Fe-2S] cluster synthesis for the human Fe–S assembly complex. Our study also tells a cautionary tale of the complexities of Fe–S chemistry that could easily mislead unsuspecting researchers who study Fe–S cluster assembly or chemically reconstitute recombinant Fe–S proteins.

Supplementary Material

Refer to Web version on PubMed Central for supplementary material.

Acknowledgments

Funding

This work was supported in part by Texas A&M University, Robert A. Welch Foundation Grant A-1647 (D.P.B.), and National Institutes of Health Grants GM096100 (D.P.B.) and GM084266 (P.A.L.).

We thank Christopher D. Putnam, James Vranish, D. J. Martin, and Seth Cory for helpful discussion and suggestions. We also thank John Markley for the gift of the FDX1 plasmid.

ABBREVIATIONS

CD	circular dichroism
DTT	dithiothreitol
EDTA	ethyl-enediaminetetraacetic acid
EPR	electron paramagnetic resonance
FDX1	ferredoxin
FXN	frataxin
GSH	glutathione
HMWS	high-molecular weight species
IPTG	isopropyl β-D-1-thiogalactopyranoside
ISC	iron–sulfur cluster
LMWS	low-molecular weight species
SD	protein complex composed of NFS1 and ISD11
SDU	protein complex composed of SD and ISCU2
SDUF	protein complex composed of SDU and frataxin

References

1. Johnson DC, Dean DR, Smith AD, Johnson M. Structure, function, and formation of biological iron-sulfur clusters. Annu Rev Biochem. 2005; 74:247–281. [PubMed: 15952888]
2. Lill R. Function and biogenesis of iron-sulphur proteins. Nature. 2009; 460:831–838. [PubMed: 19675643]
3. Rouault TA, Tong WH. Iron-sulfur cluster biogenesis and human disease. Trends Genet. 2008; 24:398–407. [PubMed: 18606475]
4. Pierik AJ, Netz DJA, Lill R. Analysis of iron-sulfur protein maturation in eukaryotes. Nat Protoc. 2009; 4:753–766. [PubMed: 19528951]
5. Lill R, Mühlenhoff U. Maturation of Iron-Sulfur Proteins in Eukaryotes: Mechanisms, Connected Processes, and Diseases. Annu Rev Biochem. 2008; 77:22.21–22.32.
6. Sheftel AD, Lill R. The power plant of the cell is also a smithy: The emerging role of mitochondria in cellular iron homeostasis. Ann Med. 2009; 41:82–99. [PubMed: 18720092]
7. Lill R, Mühlenhoff U. Iron-sulfur protein biogenesis in eukaryotes: Components and mechanisms. Annu Rev Cell Dev Biol. 2006; 22:457–486. [PubMed: 16824008]
8. Beinert H, Holm RH, Münck E. Iron-sulfur clusters: Nature's modular, multipurpose structures. Science. 1997; 277:653–659. [PubMed: 9235882]

9. Zheng L, White RH, Cash VL, Dean DR. Mechanism for the desulfurization of L-cysteine catalyzed by the nifS gene product. Biochemistry. 1994; 33:4714–4720. [PubMed: 8161529]
10. Behshad E, Bollinger J. Kinetic Analysis of Cysteine Desulfurase CD0387 from *Synechocystis* sp PCC 6803: Formation of the Persulfide Intermediate. Biochemistry. 2009; 48:12014–12023. [PubMed: 19883076]
11. Behshad E, Parkin SE, Bollinger JM. Mechanism of cysteine desulfurase Slr0387 from *Synechocystis* sp. PCC 6803: Kinetic analysis of cleavage of the persulfide intermediate by chemical reductants. Biochemistry. 2004; 43:12220–12226. [PubMed: 15379560]
12. Schmucker S, Martelli A, Colin F, Page A, Wattenhofer-Donzé M, Reutenauer L, Puccio H. Mammalian Frataxin: An Essential Function for Cellular Viability through an Interaction with a Preformed ISCU/NFS1/ISD11 Iron-Sulfur Assembly Complex. PLoS One. 2011; 6:e16199. [PubMed: 21298097]
13. Wiedemann N, Urzica E, Guiard B, Muller H, Lohaus C, Meyer HE, Ryan MT, Meisinger C, Mühlenhoff U, Lill R, Pfanner N. Essential role of Isd11 in mitochondrial iron-sulfur cluster synthesis on Isu scaffold proteins. EMBO J. 2006; 25:184–195. [PubMed: 16341089]
14. Adam AC, Bornhovd C, Prokisch H, Neupert W, Hell K. The Nfs1 interacting protein Isd11 has an essential role in Fe/S cluster biogenesis in mitochondria. EMBO J. 2006; 25:174–183. [PubMed: 16341090]
15. Pandey A, Yoon H, Lyver ER, Dancis A, Pain D. Isd11p protein activates the mitochondrial cysteine desulfurase Nfs1p protein. J Biol Chem. 2011; 286:38242–38252. [PubMed: 21908622]
16. Shi Y, Ghosh M, Kovtunovych G, Crooks DR, Rouault TA. Both human ferredoxins 1 and 2 and ferredoxin reductase are important for iron-sulfur cluster biogenesis. Biochim Biophys Acta. 2012; 1823:484–492. [PubMed: 22101253]
17. Sheftel AD, Stehling O, Pierik AJ, Elsässer HP, Mühlenhoff U, Webert H, Hobler A, Hannemann F, Bernhardt R, Lill R. Humans possess two mitochondrial ferredoxins, Fdx1 and Fdx2, with distinct roles in steroidogenesis, heme, and Fe/S cluster biosynthesis. Proc Natl Acad Sci USA. 2010; 107:11775–11780. [PubMed: 20547883]
18. Webert H, Freibert SA, Gallo A, Heidenreich T, Linne U, Amlacher S, Hurt E, Muhlenhoff U, Banci L, Lill R. Functional reconstitution of mitochondrial Fe/S cluster synthesis on Isu1 reveals the involvement of ferredoxin. Nat Commun. 2014; 5:5013. [PubMed: 25358379]
19. Uzarska MA, Dutkiewicz R, Freibert SA, Lill R, Muehlenhoff U. The mitochondrial Hsp70 chaperone Ssq1 facilitates Fe/S cluster transfer from Isu1 to Grx5 by complex formation. Mol Biol Cell. 2013; 24:1830–1841. [PubMed: 23615440]
20. Vickery L, Cupp-Vickery J. Molecular chaperones HscA/Ssq1 and HscB/Jac1 and their roles in iron-sulfur protein maturation. Crit Rev Biochem Mol Biol. 2007; 42:95–111. [PubMed: 17453917]
21. Chandramouli K, Johnson M. HscA and HscB stimulate [2Fe-2S] cluster transfer from IscU to apoferredoxin in an ATP-dependent reaction. Biochemistry. 2006; 45:11087–11095. [PubMed: 16964969]
22. Campuzano V, Montermini L, Moltè MD, Pianese L, Cossee M, Cavalcanti F, Monros E, Rodius F, Duclos F, Monticelli A, Zara F, Cañizares J, Koutnikova H, Bidichandani SI, Gellera C, Brice A, Trouillas P, De Michele G, Filla A, De Frutos R, Palau F, Patel PI, Di Donato S, Mandel JL, Cocozza S, Koenig M, Pandolfo M. Friedreich's ataxia: Autosomal recessive disease caused by an intronic GAA triplet repeat expansion. Science. 1996; 271:1423–1427. [PubMed: 8596916]
23. Tsai CL, Barondeau DP. Human frataxin is an allosteric switch that activates the Fe-S cluster biosynthetic complex. Biochemistry. 2010; 49:9132–9139. [PubMed: 20873749]
24. Bulteau AL, O'Neill HA, Kennedy MC, Ikeda-Saito M, Isaya G, Szweda LI. Frataxin acts as an iron chaperone protein to modulate mitochondrial aconitase activity. Science. 2004; 305:242–245. [PubMed: 15247478]
25. Yoon T, Cowan JA. Iron-sulfur cluster biosynthesis. Characterization of frataxin as an iron donor for assembly of [2Fe-2S] clusters in ISU-type proteins. J Am Chem Soc. 2003; 125:6078–6084. [PubMed: 12785837]
26. Kondapalli K, Kok N, Dancis A, Stemmler TL. Drosophila Frataxin: An Iron Chaperone during Cellular Fe-S Cluster Bioassembly. Biochemistry. 2008; 47:6917–6927. [PubMed: 18540637]

27. Pandey A, Yoon H, Lyver ER, Dancis A, Pain D. Identification of a Nfs1p-bound persulfide intermediate in Fe-S cluster synthesis by intact mitochondria. Mitochondrion. 2012; 12:539–549. [PubMed: 22813754]
28. Pandey A, Gordon DM, Pain J, Stemmler TL, Dancis A, Pain D. Frataxin Directly Stimulates Mitochondrial Cysteine Desulfurase by Exposing Substrate-binding Sites, and a Mutant Fe-S Cluster Scaffold Protein with Frataxin-bypassing Ability Acts Similarly. J Biol Chem. 2013; 288:36773–36786. [PubMed: 24217246]
29. Bridwell-Rabb J, Fox NG, Tsai CL, Winn AM, Barondeau DP. Human frataxin activates Fe-S cluster biosynthesis by facilitating sulfur transfer chemistry. Biochemistry. 2014; 53:4904–4913. [PubMed: 24971490]
30. Tsai CL, Bridwell-Rabb J, Barondeau DP. Friedreich's Ataxia Variants I154F and W155R Diminish Frataxin-Based Activation of the Iron-Sulfur Cluster Assembly Complex. Biochemistry. 2011; 50:6478–6487. [PubMed: 21671584]
31. Bridwell-Rabb J, Winn AM, Barondeau DP. Structure-function analysis of Friedreich's ataxia mutants reveals determinants for frataxin binding and activation of the Fe-S assembly complex. Biochemistry. 2011; 50:7265–7274. [PubMed: 21776984]
32. Colin F, Martelli A, Clemancey M, Latour JM, Gambarelli S, Zeppieri L, Birck C, Page A, Puccio H, Ollagnier de Choudens S. Mammalian Frataxin Controls Sulfur Production and Iron Entry during de Novo Fe_4S_4 Cluster Assembly. J Am Chem Soc. 2013; 135:733–740. [PubMed: 23265191]
33. Agar J, Krebs C, Frazzon J, Huynh BH, Dean DR, Johnson M. IscU as a scaffold for iron-sulfur cluster biosynthesis: Sequential assembly of [2Fe-2S] and [4Fe-4S] clusters in IscU. Biochemistry. 2000; 39:7856–7862. [PubMed: 10891064]
34. Mühlenhoff U, Richter N, Pines O, Pierik AJ, Lill R. Specialized function of yeast Isa1 and Isa2 proteins in the maturation of mitochondrial [4Fe-4S] proteins. J Biol Chem. 2011; 286:41205–41216. [PubMed: 21987576]
35. Adinolfi S, Iannuzzi C, Prischi F, Pastore C, Iametti S, Martin S, Bonomi F, Pastore A. Bacterial frataxin CyaY is the gatekeeper of iron-sulfur cluster formation catalyzed by IscS. Nat Struct Mol Biol. 2009; 16:390–396. [PubMed: 19305405]
36. Kim JH, Tonelli M, Markley JL. Disordered form of the scaffold protein IscU is the substrate for iron-sulfur cluster assembly on cysteine desulfurase. Proc Natl Acad Sci USA. 2012; 109:454–459. [PubMed: 22203963]
37. Huang J, Cowan JA. Iron-sulfur cluster biosynthesis: Role of a semi-conserved histidine. Chem Commun. 2009; 21:3071–3073.
38. Bridwell-Rabb J, Iannuzzi C, Pastore A, Barondeau DP. Effector role reversal during evolution: The case of frataxin in Fe-S cluster biosynthesis. Biochemistry. 2012; 51:2506–2514. [PubMed: 22352884]
39. Xia B, Cheng H, Bandarian V, Reed GH, Markley JL. Human ferredoxin: Overproduction in *Escherichia coli*, reconstitution in vitro, and spectroscopic studies of iron-sulfur cluster ligand cysteine-to-serine mutants. Biochemistry. 1996; 35:9488–9495. [PubMed: 8755728]
40. Pagani S, Bonomi F, Cerletti P. Enzymic synthesis of the iron-sulfur cluster of spinach ferredoxin. Eur J Biochem. 1984; 142:361–366. [PubMed: 6430704]
41. Marelja Z, Stöcklein W, Nimtz M, Leimkühler S. A novel role for human Nfs1 in the cytoplasm: Nfs1 acts as a sulfur donor for MOCS3, a protein involved in molybdenum cofactor biosynthesis. J Biol Chem. 2008; 283:25178–25185. [PubMed: 18650437]
42. Siegel LM. A direct microdetermination for sulfide. Anal Biochem. 1965; 11:126–132. [PubMed: 14328633]
43. Fish WW. Rapid Colorimetric Micromethod for the Quantitation of Complexed Iron in Biological Samples. Methods Enzymol. 1988; 158:357–364. [PubMed: 3374387]
44. Stookey L. Ferrozine: A new spectrophotmetric reagent for iron. Anal Chem. 1970; 42:779–781.
45. Cowart RE, Singleton FL, Hind JS. A comparison of bathophenanthrolinedisulfonic acid and ferrozine as chelators of iron(II) in reduction reactions. Anal Biochem. 1993; 211:151–155. [PubMed: 8323027]

46. Gao HY, Subramanian S, Couturier J, Naik SG, Kim SK, Leustek T, Knaff DB, Wu HC, Vignols F, Huynh BH, Rouhier N, Johnson MK. *Arabidopsis thaliana* Nfu2 Accommodates [2Fe-2S] or [4Fe-4S] Clusters and Is Competent for in Vitro Maturation of Chloroplast [2Fe-2S] and [4Fe-4S] Cluster-Containing Proteins. Biochemistry. 2013; 52:6633–6645. [PubMed: 24032747]
47. Bonomi F, Iametti S, Morleo A, Ta D, Vickery LE. Facilitated Transfer of IscU-[2Fe2S] Clusters by Chaperone-Mediated Ligand Exchange. Biochemistry. 2011; 50:9641–9650. [PubMed: 21977977]
48. Mansy SS, Wu G, Surerus KK, Cowan JA. Iron-sulfur cluster biosynthesis *Thermatoga maritima* IscU is a structured iron-sulfur cluster assembly protein. J Biol Chem. 2002; 277:21397–21404. [PubMed: 11934893]
49. Mapolelo DT, Zhang B, Naik SG, Huynh BH, Johnson MK. Spectroscopic and functional characterization of iron-sulfur cluster-bound forms of *Azotobacter vinelandii* (Nif)IscA. Biochemistry. 2012; 51:8071–8084. [PubMed: 23003323]
50. Ryle MJ, Lanzilotta WN, Seefeldt LC, Scarrow RC, Jensen GM. Circular dichroism and X-ray spectroscopies of *Azotobacter vinelandii* nitrogenase iron protein. MgATP and MgADP induced protein conformational changes affecting the [4Fe-4S] cluster and characterization of a [2Fe-2S] form. J Biol Chem. 1996; 271:1551–1557. [PubMed: 8576152]
51. Agar JN, Krebs C, Frazzon J, Huynh BH, Dean DR, Johnson MK. IscU as a scaffold for iron-sulfur cluster biosynthesis: Sequential assembly of [2Fe-2S] and [4Fe-4S] clusters in IscU. Biochemistry. 2000; 39:7856–7862. [PubMed: 10891064]
52. Qi W, Li J, Chain CY, Pasquevich GA, Pasquevich AF, Cowan JA. Glutathione complexed Fe-S centers. J Am Chem Soc. 2012; 134:10745–10748. [PubMed: 22687047]
53. Garg VK. Mössbauer studies of iron sulphide minerals. Rev Bras Fis. 1980; 10:535–558.
54. Chakrabarti, M.; Lindahl, PA. The utility of Mössbauer spectroscopy in eukaryotic cell biology and animal physiology. In: Rouault, TA., editor. Iron Sulfur Clusters in Chemistry and Biology. Walter de Gruyter; Berlin: 2014. p. 49-75.
55. Lanz ND, Grove TL, Gogonea CB, Lee KH, Krebs C, Booker SJ. RlmN and AtsB as models for the overproduction and characterization of radical SAM proteins. Methods Enzymol. 2012; 516:125–152. [PubMed: 23034227]
56. Que L, Holm RH, Mortenson LE. Extrusion of Fe_2S_2 and Fe_4S_4 Cores from Active-Sites of Ferredoxin Proteins. J Am Chem Soc. 1975; 97:463–464. [PubMed: 1133364]
57. Vranish JN, Russell WK, Yu LE, Cox RM, Russell DH, Barondeau DP. Fluorescent probes for tracking the transfer of iron-sulfur cluster and other metal cofactors in biosynthetic reaction pathways. J Am Chem Soc. 2015; 137:390–398. [PubMed: 25478817]

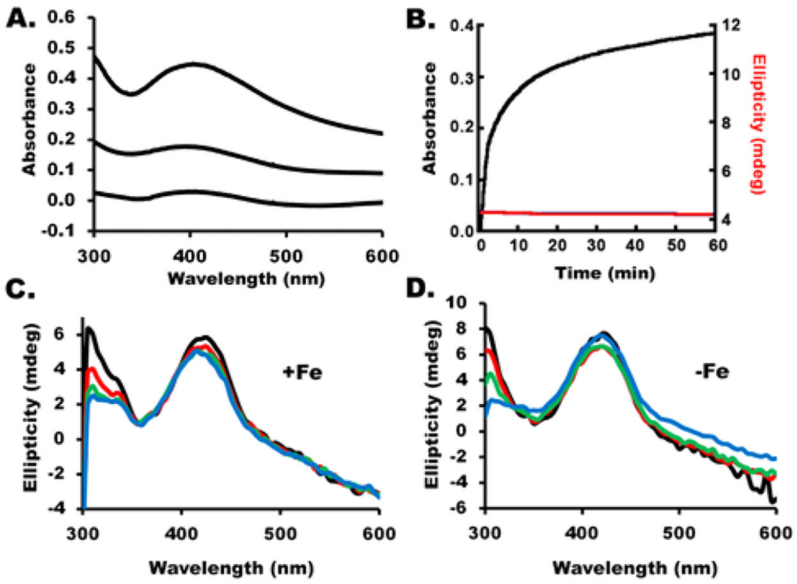

Figure 1.

SDUF complex generates Fe–S species under standard conditions with spectroscopic properties similar to those of [4Fe-4S] clusters. (A) Absorbance spectrum of the SDUF reaction mixture 45 s (bottom), 2.8 min, and 1 h (top) after the reaction was initiated. (B) Kinetics of the assembly assay reaction monitored by absorbance at 400 nm (black) and CD ellipticity at 430 nm (red). The absorbance was adjusted to zero at 0 min. (C) CD spectra of the reaction mixture recorded at 0 (black), 20 (red), 40 (green), and 90 (blue) min. (D) CD spectra of an equivalent reaction mixture as in C except that it included 10 mM EDTA and excluded Fe^{2+}. Spectra were recorded at 0 (black), 10 (red), 20 (green), and 40 (blue) min.

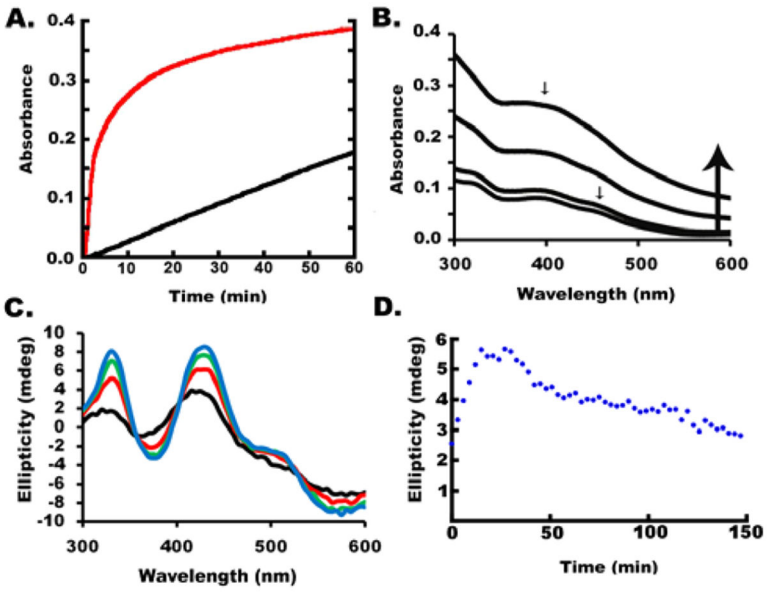

Figure 2.

SDU complex generates [2Fe-2S] clusters under standard conditions. (A) Comparison of the change in absorbance at 456 nm for the SDU (black) and SDUF (red) complexes. (B) Absorbance spectrum for the SDU reaction mixture recorded at 5, 10, 30, and 60 min. The small arrow at 456 nm highlights the formation of [2Fe-2S] clusters at early times, while the arrow at 400 nm highlights features similar to those of the SDUF reaction (Figure 1A) at later times. (C) CD spectra recorded for the SDU reaction at 0 (black), 20 (red), 40 (green), and 90 (blue) min. The features at 330 and 430 nm are assigned to [2Fe-2S]-ISCU2. (D) Time-dependent changes in 330 nm ellipticity for a separate SDU reaction under standard conditions.

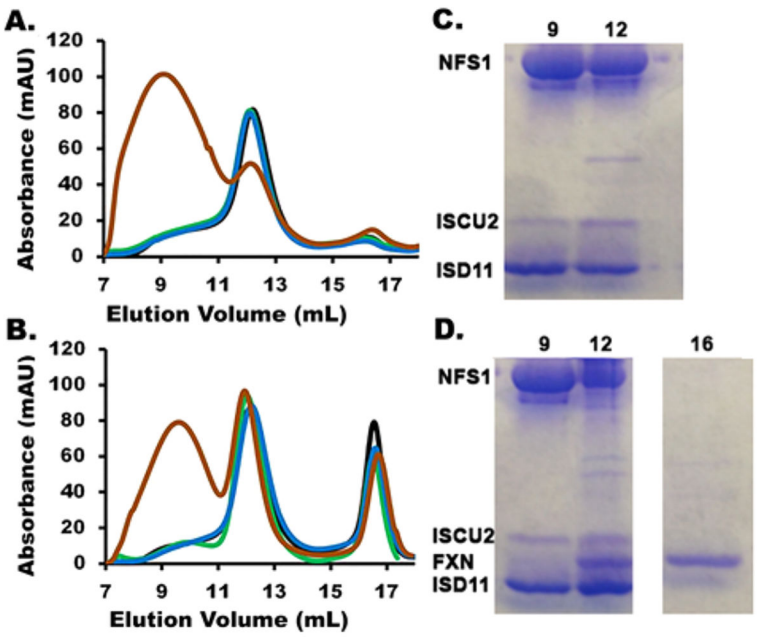

Figure 3.

HMWS formation during Fe–S cluster assembly reactions under standard conditions. Size-exclusion chromatogram, monitored at A_{280}, of reaction mixtures involving (A) SDU and (B) SDUF under complete standard conditions (brown) but lacking cysteine (green), Fe^{2+} (blue), or both cysteine and Fe^{2+} (black). SDS–PAGE of fractions from Fe–S cluster assembly reactions involving (C) SDU and (D) SDUF. Fractions 9 (void), 12 (native SD, SDU, and SDUF), and 16 mL (uncomplexed ISCU2 and FXN) from anaerobic S-200 columns were analzyed by SDS–PAGE. The gel was stained with Coomassie Blue. Migration positions of NSF1, ISCU2, FXN, and ISD11 are shown.

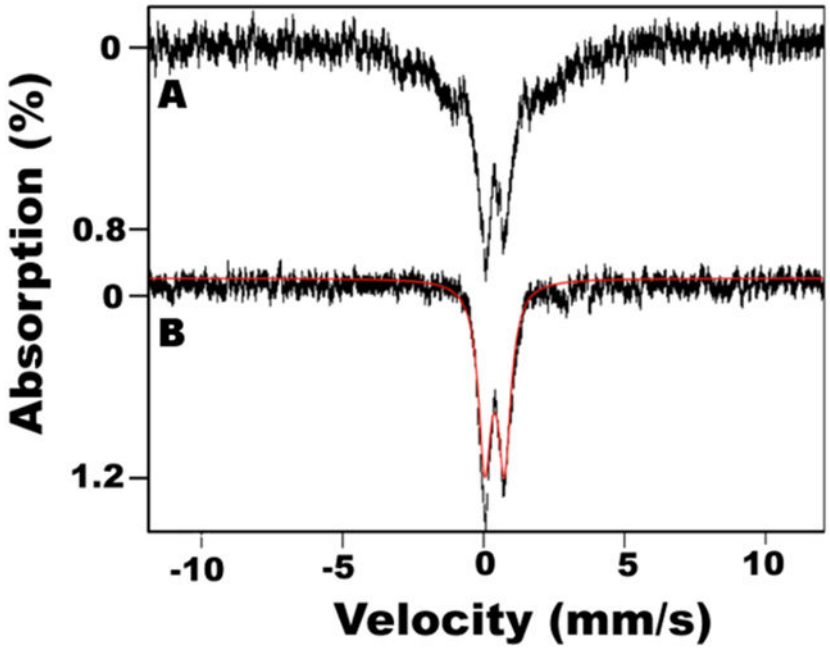

Figure 4.

Mössbauer spectra of the HMWS mineral. The HMWS was generated with the SD complex under standard conditions and isolated from the void volume fractions of the S-200 column. Low-field (0.05 T) Mössbauer spectra were recorded at (A) 5 and (B) 100 K. The solid red line overlaying the data is a simulation of the quadrupole doublet due to the HMWS.

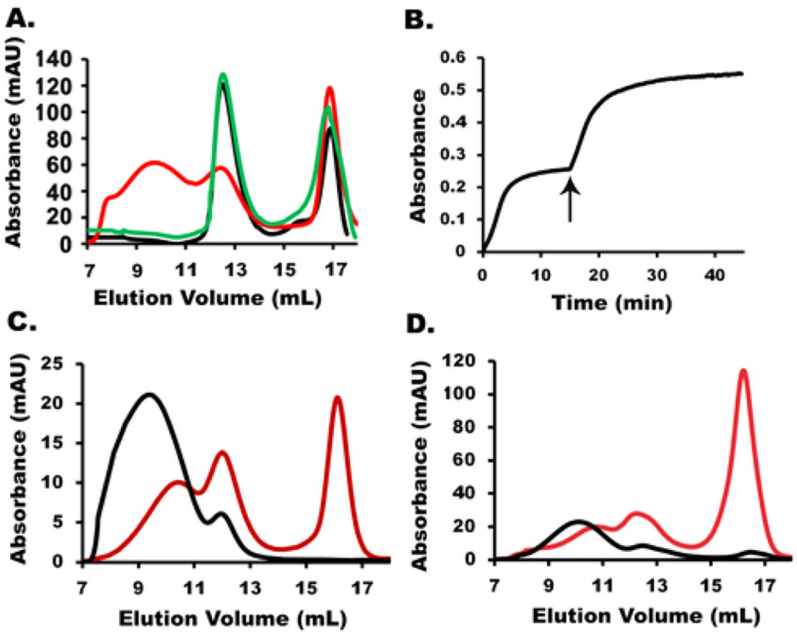

Figure 5.

Formation conditions and reaction properties of HMWS. (A) Size-exclusion chromatogram, monitored at A_{280}, of the SDUF complex incubated with DTT and S^{2-} (black), Fe^{2+} and S^{2-} (red), or Fe^{2+} and S^{2-} using an SDUF complex in which NSF1 had been alkylated (green). (B) Kinetics of SDUF Fe–S cluster assembly reaction under standard conditions spiked (arrow) with 100 μM L-cysteine show that the plateau in 400 nm absorbance is due to depletion of cysteine/sulfide. (C) Size-exclusion chromatogram, monitored at A_{405}, of the reaction mixture involving the SDUF complex in the absence (black) or presence (red) of apo-FDX1. (D) Size-exclusion chromatogram, monitored by absorbance at A_{405}, of the isolated HMWS with (red) or without (black) added apo-FDX1.

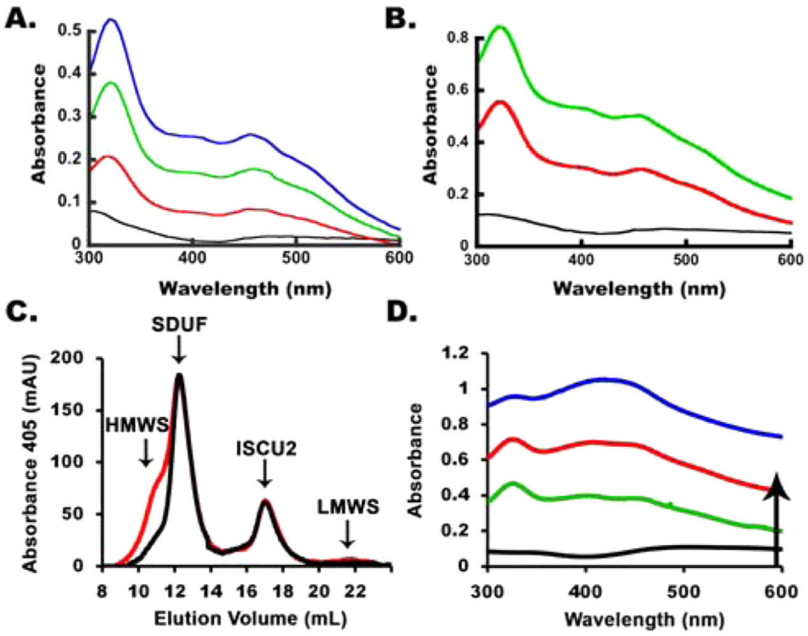

Figure 6.

Fe–S cluster assembly reactions under DTT-free conditions generate [2Fe-2S] clusters and delay HMWS formation. (A) Absorbance spectra for SDU-catalyzed Fe–S assembly reaction after 0 (black), 30 (red) 60 (green), and 90 (blue) min. (B) Same for the SDUF-catalyzed reaction (same color coding, no 90 min spectrum). (C) Size-exclusion chromatogram, monitored at A_{405}, of the SDUF Fe–S cluster assembly reaction after 1.5 (black) and 3.5 h (red). (D) Absorbance spectra for the reaction in panel C after 0 (black), 2 (green), 3.5 (red), and 5 (blue) h.

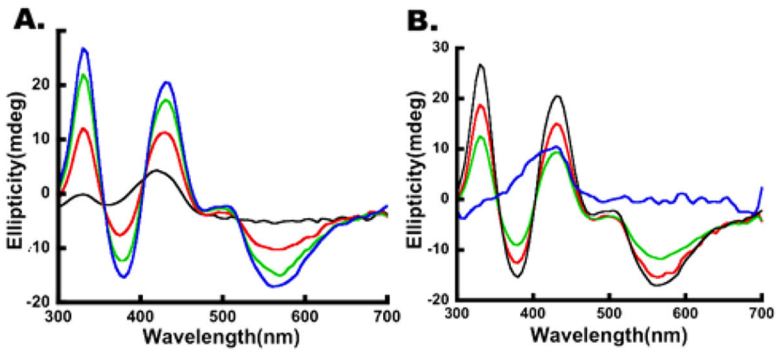

Figure 7.

Sulfide degrades [2Fe-2S] clusters bound to ISCU2. (A) Development of the [2Fe-2S] cluster CD signal after 0 (black), 30 (red), 60 (green), and 90 (blue) min for the SDU complex under DTT-free conditions. (B) Addition of 0 μM (black), 250 μM (red), 500 μM (green), and 1 mM (blue) Na_2S to the mixture for the completed reaction (90 min) from panel A.

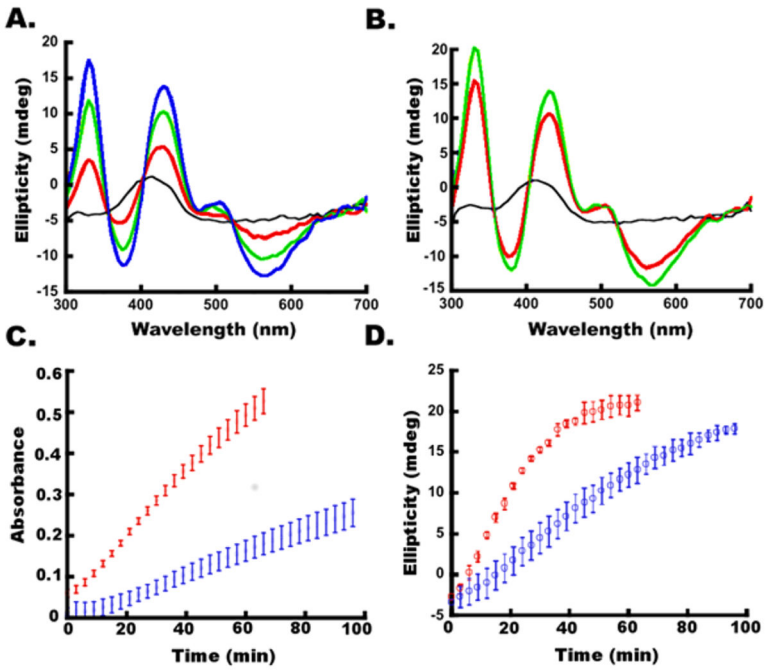

Figure 8.

FXN accelerates [2Fe-2S] cluster formation. (A) CD spectra of an SDU-catalyzed Fe–S cluster assembly reaction mixture after 0 (black), 30 (red), 60 (green), and 90 (blue) min. (B) CD spectra of an SDUF-catalyzed Fe–S assembly reaction mixture after 0 (black), 30 (red), and 60 (green) min. (C) Absorbance at 456 nm vs time of reaction for SDU-catalyzed (blue) and SDUF-catalyzed (red) reactions (shown in Figure 6A,B). (D) CD intensity at 330 nm vs time of reaction for SDU-catalyzed (blue) and SDUF-catalyzed (red) reactions. Bars are replicate errors from three experiments.

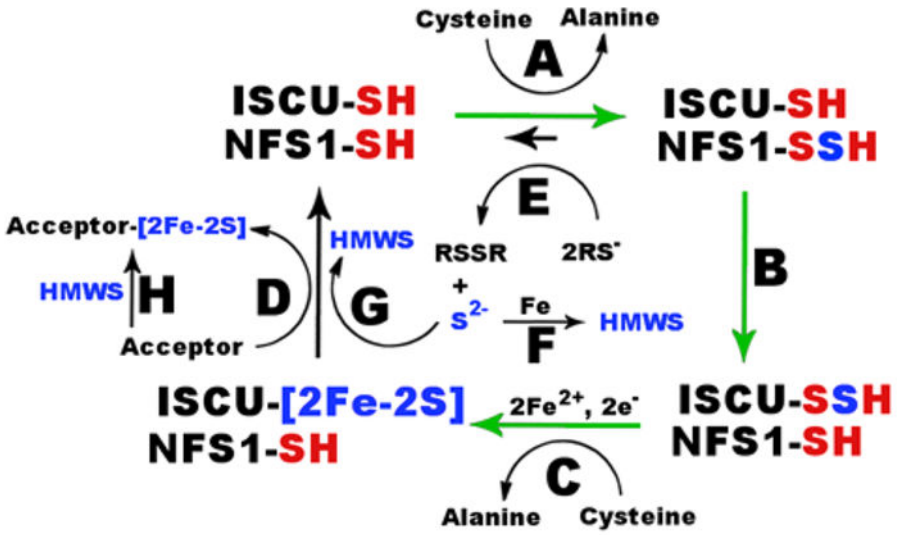

Figure 9.

Model for competing Fe–S cluster biosynthesis and mineralization pathways. (A) Generation of a persulfide intermediate on NFS1. (B) Transfer of sulfur from NFS1 to ISCU2. (C) Catalytic synthesis of a [2Fe-2S] cluster intermediate. (D) Transfer of the [2Fe-2S] cluster to apo target proteins. (E) Interception of the persulfide intermediate with reductive thiol reagents to produce sulfude. (F) Combination of sulfide, iron, and the assembly complex (not shown) to form HMWS. (G) Degradation of [2Fe-2S] intermediates by sulfide to form HMWS. (H) Chemical reconstitution of apo target protein by HMWS. FXN accelerates [2Fe-2S] cluster formation (green arrows) by the human Fe–S asembly complex.